Journal of Crystal Growth 450 (2016) 39–44

Contents lists available at ScienceDirect

Journal of Crystal Growth

journal homepage: www.elsevier.com/locate/jcrysgro

Effect of bulk growth temperature on antiphase domain boundary annihilation rate in MOCVD-grown GaAs on Si(001)

C.S.C. Barrett [a,*], T.P. Martin [a], X.-Y. Bao [b], E.L. Kennon [a], L. Gutierrez [a], P. Martin [b], E. Sanchez [b], K.S. Jones [a]

[a] Department of Materials Science and Engineering, University of Florida, Gainesville, FL 32611, USA
[b] Applied Materials, 974 East Arques Avenue, Sunnyvale, CA 94085, USA

ARTICLE INFO

Article history:
Received 20 April 2016
Received in revised form
13 June 2016
Accepted 14 June 2016
Available online 16 June 2016

Keywords:
A1. Planar defects
A3. Metalorganic chemical vapor deposition
B2. Semiconducting gallium arsenide
B2. Semiconducting III–V materials

ABSTRACT

GaAs is a material of interest as a potential buffer layer in future III–V semiconductor-based transistor technologies integrated on Si wafers. The goal of this study was to investigate the effect of growth temperature on the propagation and annihilation of antiphase domain boundaries (APBs) in GaAs films grown on Si(001) by metal-organic chemical vapor deposition (MOCVD). No intentional wafer off-cuts or high temperature pre-growth anneals (> 1000 °C) were employed as both of these practices complicate integration with other devices. To evaluate the role of growth temperature on the APB evolution, a 200 nm thick layer of GaAs was grown on the Si at a fixed temperature of 530 °C so that all samples started with the same approximate APB density. Subsequently, 600 nm of GaAs was grown at temperatures varying between 530 °C and 650 °C. Chemical etching combined with scanning electron microscopy (SEM) was used to profile the density of the APBs in each sample as a function of depth. The APB annihilation rate, i.e. the exponential decay rate of APB density with respect to film thickness, increases from 2.6 μm^{-1} to 10.7 μm^{-1} as the growth temperature increases from 530 °C to 610 °C and then saturates. The increase in annihilation rate with increasing temperatures suggests that the higher temperatures remove kinetic barriers to the reduction of the overall APB interfacial area. An activation energy of 1.1 eV was extracted using an Arrhenius relationship and likely corresponds to the energy needed for APBs to kink from {110} to higher-index planes, e.g. {112}. Dark field transmission electron microscopy showed that at higher growth temperatures the APBs can shift from vertical {110} habit planes to {112} planes leading to self-annihilation with sufficient thickness.

1. Introduction

The drive for continued improvements in the electrical performance and power-efficiency of complementary metal oxide semiconductor (CMOS) devices at ever-decreasing physical length scales has spurred interest in the use of III–V compound semiconductors to replace Si. III–V materials such as InGaAs or InAs are particularly attractive alternatives to Si for future n-channel devices because of their potential for much higher electron mobilities and injection velocities [1]. Integration of III–V devices on Si wafers will make large-scale production much more economically viable. Thus, significant effort has been directed towards obtaining high-quality III–V epitaxial layers on Si. The electrical and optical properties of these layers are often degraded by growth-related defects such as threading dislocations stemming from lattice constant mismatch or antiphase domain boundaries (APBs) from the polar-on-nonpolar growth [2].

Various strategies have been developed with the aim of decreasing the overall number of defects in III–V films grown on Si. Threading dislocation density can be reduced through the use of buffer layers to alleviate lattice strain [3–6]. GaAs is a good candidate for a buffer layer material because of its intermediate lattice constant between InGaAs/InAs and Si and so it is important to first obtain high-quality epitaxy of GaAs on Si. APBs are known to form in III–V epitaxial films on Si due to steps on the Si surface a single atom in height that disrupt the ordering of atoms in the III–V layer. Similar atoms become bonded to each other, such as Ga–Ga and As–As in GaAs, forming a plane of antisite defects constituting the APB. Reduction of the APB density is therefore typically accomplished through substrate preparation techniques that induce a double-step reconstruction of the (001) Si surface such as high-temperature pre-growth anneals near 1000 °C [7–9] or off-cutting the wafer towards a given direction, usually $<110>$ type [10].

* Corresponding author.
E-mail address: cscbarrett@ufl.edu (C.S.C. Barrett).

http://dx.doi.org/10.1016/j.jcrysgro.2016.06.021
0022-0248/

Having a completely double-stepped Si surface can theoretically prevent the nucleation of any APBs. However, these two strategies should be avoided for conventional CMOS processing as lower thermal budgets are required and nominally planar wafers are necessary to maintain compatibility with existing tools and procedures.

It is apparent that complete prevention of APB nucleation is not feasible through currently established methods. Thus, it becomes critical to understand the factors that influence the propagation of APBs in order to facilitate self-annihilation. Calculations of APB energetics in GaAs indicate that {110} APBs which are orthogonal to a (001) substrate have the lowest formation energy compared to APBs on higher-index planes such as {111} or {112} which are inclined relative to the substrate normal [11,12]. Clearly, {110} oriented APBs are not conducive for self-annihilation. However, it has been observed experimentally with transmission electron microscopy (TEM) that while APBs in GaAs typically form along {110} planes they have a tendency to change their plane of propagation during growth [13–17]. Georgakilas et al., also analyzed the through-thickness APB density in a GaAs film grown on Si and found that the APB density decreased with increasing distance from the GaAs/Si interface, an indirect indication that the APBs were propagating along inclined planes and self-annihilating [17]. Propagation along {112} planes may be favorable over other higher-index planes for APB annihilation since stoichiometry is maintained, as is the case with {110} APBs [12].

One factor that may influence the preferred plane of propagation for APBs is the growth temperature of the film. It has been demonstrated in GaP-on-Si that an increase in the bulk growth temperature can cause APBs to change from being majority {110} oriented to majority {111} and {112} oriented [18,19]. This effect has not yet been studied for GaAs-on-Si and the effect of growth temperature on APB annihilation has not been quantified. It is also unclear why higher growth temperatures appear to favor APB orientations that are nominally higher in formation energy. It is plausible that the kinking of APBs from {110} to higher-index planes is a thermally-activated process driven by a consequential reduction in APB interfacial area. The aim of this work is to conclusively analyze the effect of growth temperature on propagation and annihilation of APBs in GaAs grown on Si via metal-organic chemical vapor deposition (MOCVD) and to gain insight on the associated APB energetics.

2. Experimental

All GaAs film growth was carried out in an industrial III–V MOCVD system. The substrates were 300 mm (001) Si wafers with no intentional off-cut. The uncertainty of the wafer orientation is typically within a few tenths of a degree, within industry tolerances. Different batches of Si substrates have not been observed to have a significant effect on APB density in the GaAs films. Native oxide was removed from the wafers prior to film growth in a selective process that has been discussed elsewhere [20]. The wafers were then transferred under vacuum to the MOCVD growth chamber where a >800 °C bake was applied to promote the formation of double-steps. To prevent potential contamination from desorption of volatile species on the chamber walls, the reactor was first baked at a high temperature prior to the transfer of the wafers. The substrate preparation procedure reduces the density of APBs in the GaAs films by over an order of magnitude [20]. In addition to being beneficial from a defect-suppression standpoint, a low APB density is useful in this study because when the APB density is very high it becomes difficult to detect any significant changes in density over the thickness of the film.

GaAs epitaxy on Si was carried out in the standard two-step manner with a low temperature nucleation and high temperature bulk growth to improve crystal quality [21,22]. The precursors for Ga and As were trimethylgallium (TMGa) and tertiarybutylarsine (TBAs), respectively. Other growth conditions such as chamber pressure and V/III ratio were within the range of typical MOCVD process conditions. For the purposes of this study, the nucleation layer consisted of 200 nm of GaAs grown at 530 °C for all samples. This step allowed for the same approximate APB density to be set across the samples. Subsequently, 600 nm of the high temperature bulk layer was grown with varying temperature from 530 °C to 650 °C to analyze the effect of increasing growth temperature on APB propagation and annihilation. No other growth conditions were changed.

The through-thickness APB density for each sample was analyzed using a similar method to that presented by Georgakilas et al. [17]. A CH_3OH:H_3PO_4(85%):H_2O_2(30%) (10:1:1) etchant was used to remove some thickness of GaAs without selectively etching defects. Film thicknesses of samples after the H_3PO_4 etch were measured with a JA Woollam M88 ellipsometer. Subsequently, samples were dipped in a HF(49%):HNO_3(69%):H_2O (10:1:3) solution for a short time (<10 s) to selectively etch APBs. This HF/HNO_3 etchant has been previously shown to be selective for APBs in GaAs [13,17,20,23] and can therefore improve contrast in imaging and differentiate APBs from other features. Images of the sample surfaces in various areas were taken in plan view with a FEI Nova NanoSEM 430 scanning electron microscope (SEM) operating at 5 kV. APB densities were determined by tracing APB features in SEM images with ImageJ software [24]. The APB density is defined as the line length of APBs per unit area, giving units of μm^{-1}. The minimum size of APBs that can be detected through this method is on the order of 0.1–0.2 μm in circumference, based on the minimum value of APB lengths that were collected.

The evolution of APB propagation in the samples was analyzed through cross-sectional TEM (XTEM). A JEOL 200CX TEM operating at 200 kV was used. XTEM specimens were prepared in $<110>$ orientations using a FEI DB325 focused ion beam (FIB) instrument. Dark field imaging was performed with the (002) and $(00-2)$ superlattice reflections in order to have sensitivity for crystal orientation across antiphase domains (APDs) [25–29]. Further tilting of the samples off of the $[-110]$ zone axis to excite the (115) and $(11-7)$ spots increases the intensity of the (002) reflection [18]. Under these conditions, APDs will have opposing contrast relative to the surrounding GaAs crystal. Thus the shape of a domain can be observed including the planes of propagation for the bounding APBs.

3. Results and discussion

Fig. 1 shows representative plan view SEM images of two specimens of the sample with a bulk layer grown at 570 °C after etching down to a GaAs film thickness of 745 nm (a) and 240 nm (b), corresponding to APB densities of 0.047 ± 0.017 μm^{-1} and 0.33 ± 0.06 μm^{-1}, respectively. The type of discrete APDs with faceting observed in Fig. 1 was typical for all samples. It is evident from the images in Fig. 1 that the number of visible APDs is decreasing with increasing film thickness. Therefore, APBs must be kinking to higher-index planes and annihilating during growth leading to the termination of a significant portion of domains. A similar trend was observed in the other samples with varied bulk layer temperature. This result is not in itself surprising after the Georgakilas et al., study [17] showed a decrease of APB density with increasing film thickness in GaAs-on-Si. However, the presence of discrete APDs versus long, extended APBs allows for a clear visual demonstration of the tendency for APBs to annihilate.

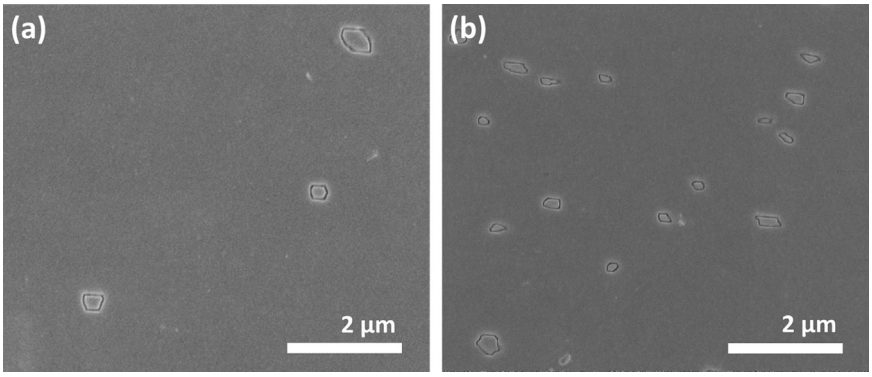

Fig. 1. Plan view SEM images of sample grown with a bulk layer at 570 °C at a film thickness of 745 nm (a) and 240 nm (b). The corresponding APB densities for these specimens are $0.047 \pm 0.017\ \mu m^{-1}$ (a) and $0.33 \pm 0.06\ \mu m^{-1}$ (b). There is a clear decrease in the number of antiphase domains with increasing film thickness. The specimens were stained with the HF/HNO_3 solution to improve APB contrast.

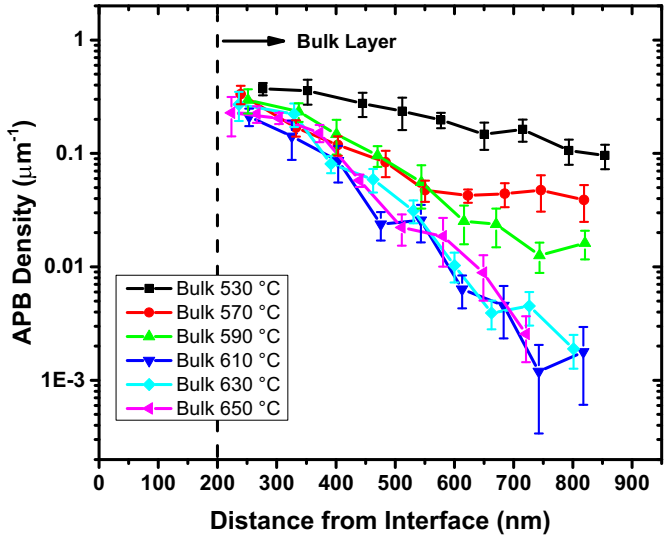

Fig. 2. Plot of through-thickness APB density for all GaAs-on-Si samples with varied bulk layer growth temperature. APB density decreases during growth due to APB kinking and annihilation. The annihilation rate with respect to film thickness is enhanced by increasing the bulk layer temperature up to 610 °C.

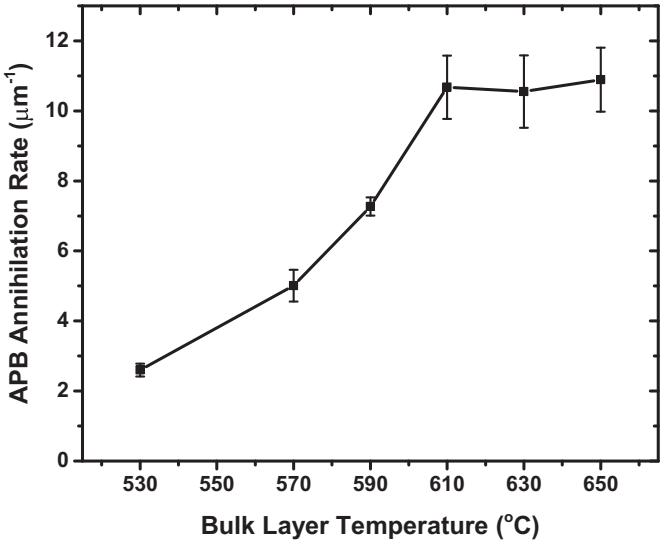

Fig. 3. Plot of APB annihilation rate with respect to film thickness for all samples versus bulk layer growth temperature. Annihilation rate increases with increasing temperature until saturation at 610 °C.

The through-thickness APB density profiles for all samples are shown in Fig. 2. Final film thicknesses did vary slightly as each sample spent the same amount of time at its respective growth temperature and no other growth conditions were changed. There is a decrease in APB density for each sample with increasing distance from the GaAs/Si interface, i.e. as GaAs film thickness increases during growth. The decrease in density stems from a decrease in the total line length of APBs in the (001) growth plane as the APBs kink to higher-index planes and annihilate. The sample with the bulk layer growth at 530 °C, identical in temperature to the nucleation layer, was grown to control for thickness effects and experienced a relatively moderate decrease in APB density. While this sample shows there is an inherent tendency for APB annihilation with increasing growth thickness, increasing the bulk layer temperature to 570, 590, and 610 °C causes an apparent increase in the rate that the APB density decreases with respect to film thickness. There is no apparent enhancement of the APB annihilation rate with respect to film thickness after raising the bulk layer temperature above 610 °C, i.e. the samples at 630 and 650 °C follow the same approximate curve as 610 °C.

Since the through-thickness APB density profiles of the samples in Fig. 2 follow an exponential decay, the APB annihilation rate can be extracted. The curves were fit to a standard exponential decay equation as a function of GaAs film thickness. The APB annihilation rate was defined as the exponential decay rate of APB density with respect to film thickness, giving units of μm^{-1}. In other words, a greater annihilation rate corresponds to a smaller film thickness required to completely annihilate APBs. Fig. 3 plots the calculated APB annihilation rates versus the bulk layer temperature for all samples. The APB annihilation rate increases with increasing bulk layer temperature from 530 °C to 610 °C by approximately a factor of four from $2.6 \pm 0.2\ \mu m^{-1}$ to $10.7 \pm 0.9\ \mu m^{-1}$. After 610 °C, the annihilation rate saturates. The strong correlation between the bulk layer temperature and the APB annihilation rate, combined with the knowledge that all samples were grown with identical nucleation layers, indicates that a greater overall number of APBs are able to change their plane of propagation and annihilate at higher growth temperatures. Thus, the kinking of APBs to higher-index planes may be mediated by a thermally-activated process. The saturation of APB annihilation rate at higher growth temperatures likely arises from geometric factors, i.e. the plane of propagation for annihilation. If a given family of planes is preferred energetically, e.g. {112} over {111} or {113}, to achieve annihilation, then the annihilation rate is ultimately limited by the number of APBs that kink to this plane.

Dark field XTEM images of APBs in the GaAs film are shown in Figs. 4 and 5. Fig. 4 shows an APD in the sample grown with the bulk layer at 630 °C in dark field under (002) (a) and (00-2) (b) conditions. The reversal of contrast within the domain from

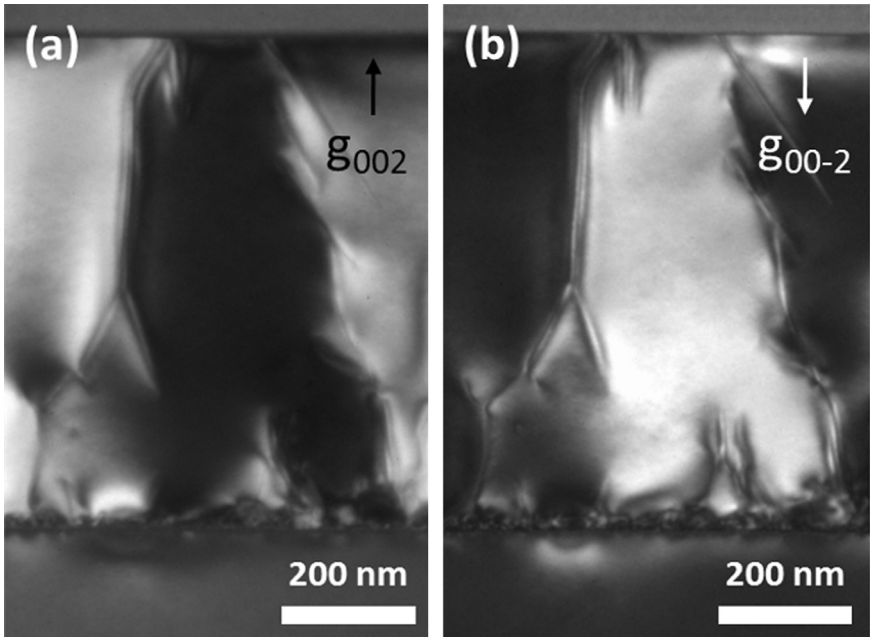

Fig. 4. Dark field-XTEM images of an APD in the sample with bulk layer grown at 630 °C using (002) (a) and (00-2) (b) reflections. The reversal of contrast within the APD relative to the surrounding crystal from (a) to (b) demonstrates this is an APD.

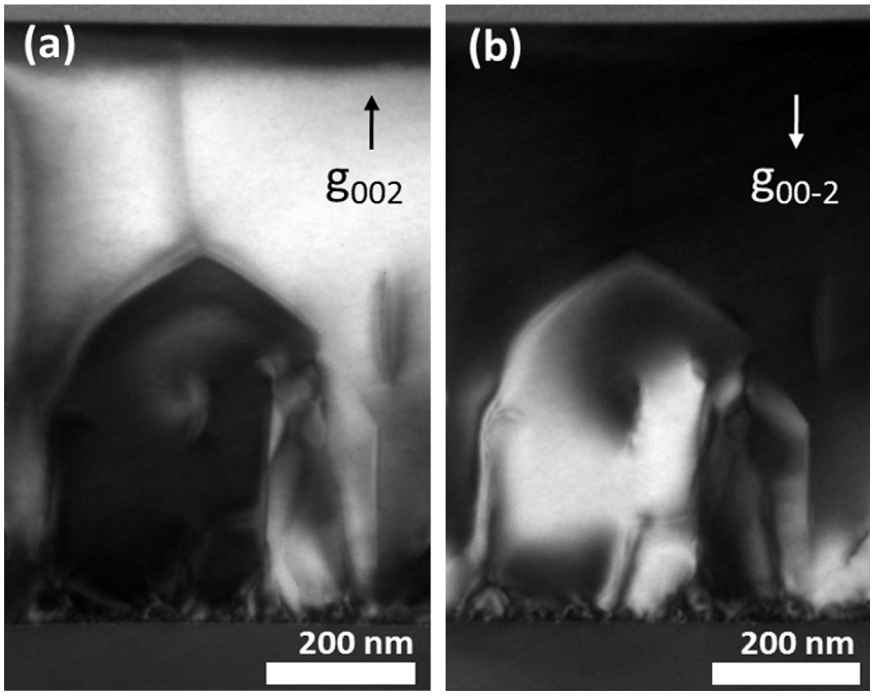

Fig. 5. Dark field-XTEM images of the sample with bulk layer grown at 610 °C using (002) (a) and (00-2) (b) reflections showing an APD terminating within the GaAs layer. The angle of APB annihilation is consistent with {112} type planes.

Fig. 4(a) to (b) confirms that this is an APD. The width of the domain is on the order of those typically observed in plan-view SEM (Fig. 1). While the APD is not completely suppressed in the film, the width of the APD does decrease during growth. The reduction in width allows for a corresponding reduction in APB interfacial area. The habit planes of the APBs are varied and difficult to distinguish, but the shrinking width of the domain indicates a tendency towards higher-index planes. Fig. 5 shows a section of the sample grown with the bulk layer at 610 °C containing a self-annihilating APD under (002) (a) and (00-2) (b) dark field conditions. The APBs initiate in a mostly vertical direction along {110} planes before annihilating. The terminating APBs lie at an angle of approximately 35° relative to the (001) growth plane, indicating that these are {112} APBs. Thus, {112} can become a favorable plane of propagation over {110} to facilitate APB annihilation. In fact, Beyer et al., reported the preferential annihilation along {112} planes in a GaP-on-Si system under optimized growth conditions with bulk growth at 675 °C [30]. The kinking of APBs to higher-index planes such as {112} at lower growth temperatures is likely limited by a kinetic barrier.

The activation energy for the kinking of APBs to higher-index planes can be determined through an Arrhenius relationship. Fig. 6

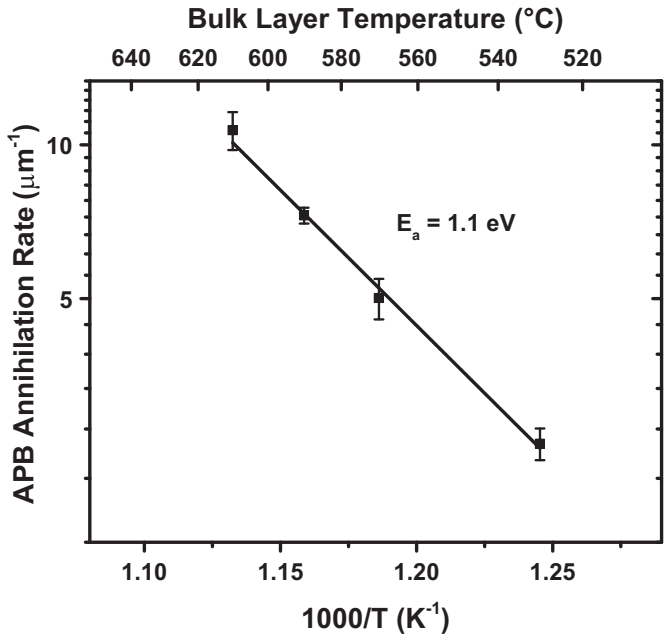

Fig. 6. Arrhenius plot of APB annihilation rate versus inverse bulk layer growth temperature. The activation energy was found to be 1.1 eV. This energy is representative of the barrier for APBs kinking to higher-index planes and annihilating.

shows the APB annihilation rates for the samples with bulk layer growth at 530, 570, 590, and 610 °C (i.e., before saturation of annihilation rate) on an Arrhenius plot. The activation energy was calculated to be 1.1 eV. It is possible that the activation energy is related to the energy required to form the additional wrong bonds in a {112} APB configuration versus a {110} configuration. As a reference, the wrong bond energy associated with antisite defects in APBs in GaAs as calculated by Rubel and Baranovskii are 0.31 eV and 0.37 eV for {110} and {112} APBs, respectively [12]. The {112} APBs also have a higher density of wrong bonds per unit area over {110} APBs [12].

Because APBs have a very large associated energy due to their structure, it follows that there is a driving force to minimize the overall area of APBs in the GaAs layer. As growth temperature is increased, the APBs in GaAs are driven towards an equilibrium configuration with orientations along higher-index planes. The thermal energy barrier explains why APBs tend to nucleate along {110} planes at lower growth temperatures. It is likely that {112} or other higher-index APBs become favored in order to reduce the line length of APBs in the (001) growth plane and thus reduce the number of adatoms involved in a given APB with each successive monolayer. This reduction in energy is balanced by the increased energy cost to form {11x} wrong bonds over {110}, where x is an integer greater than 0, to initiate the change in habit plane. As a consequence, APDs such as those seen in Fig. 1 will eventually become suppressed in the film during growth.

Another explanation for the dependence of APB annihilation rate on growth temperature is not a pure kinking of APBs to higher-index planes such as {112}, but a stepwise kinking of APBs mediated by jumps to {110} planes. In addition to showing the preferential annihilation of APBs along {112} planes [30], Beyer et al., observed that in similarly grown GaP-on-Si samples APBs oriented along {110} planes displayed a tendency to jump one or more atomic planes, thereby creating a finite thickness to the APB [31]. Thus, increasing growth temperature can increase the jump probability for APB planes and enhance the annihilation rate. However, the jumping mechanism inherently forms segments of APB facets that should be energetically unfavorable, i.e. non-stoichiometric {111} or {001}. APBs along {001} also have greater wrong bond density than {110}, {111}, or {112} [11]. It is possible that these segments are relatively small enough in length that the APB jump is still rendered favorable. Otherwise, it is unclear how a macroscopic {112} APB as observed in this study (Fig. 5) and in Ref. [30] would be manifested via the stepwise kinking mechanism. Considering the geometry of an APB in a {112} orientation, construction with {111} and {110} facets would never meet the shallow angle of a {112} plane on average. Construction with {110} and {001} facets requires that the {001} segments must be longer than the {110} segments.

APB annihilation may also be influenced by rotation of the lattice due to the differing lengths of Ga–Ga and As–As wrong bonds versus Ga–As bonds. Vajargah et al., measured phase changes in high-angle annular dark field scanning TEM (HAADF-STEM) images of a GaSb-on-Si layer and observed rotation of the lattice at an APB [32]. The rotation alternated in sequential segments which allowed the APB to initially preserve a normal direction relative to the substrate before the APB eventually kinked over to inclined planes. The authors posit that faceting along higher-index planes is influenced by this lattice rotation and local relaxation at the APB and thus it will promote annihilation. However, since the alternating rotation was seen in both the curved and normal sections of the APB, it is unclear how much effect the rotation has on the actual kinking process. As well, the change in APB formation energies along different planes due to the lattice rotation and relaxation is unknown. There may be a relationship between the local relaxation and lattice rotation at an APB and the tendency to kink to higher-index planes.

The two APB-related phenomenon discussed above in similar III–V layers to GaAs and the related experimental evidence demonstrate that the annihilation of APBs via kinking to higher-index planes is a complex process. Irrespective of the actual mechanism, there is a clear influence of growth temperature on the preference for APBs to annihilate, as shown in this study. This effect can be understood by a thermodynamic argument for the minimization of APB interfacial area in the GaAs layer. The temperature effect may at an atomic-level be related to the APB plane jumping or local lattice perturbations. The density functional theory (DFT) calculations by Rubel and Baranovskii on APB formation energies [12] are insightful but have a limited scope as only ideal systems of parallel APB planes were investigated. Additional computational work is necessary in order to fully understand the atomic mechanism that allows for APB kinking to higher-index planes to become more favorable at higher temperatures.

4. Conclusions

In summary, the annihilation rate of APBs with respect to film thickness in GaAs grown on planar (001) Si substrates has been shown to have a dependence on MOCVD growth temperature. Increasing the bulk layer growth temperature from 530 °C to 610 °C increased the exponential decay rate of APB density with respect to film thickness from 2.6 μm^{-1} to 10.7 μm^{-1}. The annihilation rate saturated after 610 °C. Dark field XTEM demonstrated that APDs have a tendency to shrink during growth and that {112} is a possible habit plane for APB annihilation at higher growth temperature. The higher growth temperatures likely remove kinetic barriers for the kinking of APBs from {110} planes to higher-index planes, e.g. {112}, to facilitate annihilation. The activation energy for APB kinking was found to be 1.1 eV which may account for the formation of additional wrong bonds to initiate the change in the plane of propagation. The kinking of APBs is likely driven by a reduction in the line length of APBs in the (001) growth plane

which reduces the number of adatoms involved in a given APB for each successive monolayer of growth. It is possible that APB jumps to adjacent {110} planes or local rotation of the lattice at the APB also play a role in facilitating annihilation. Additional computational analysis of the formation energies of complex APB systems with multiple facets is needed. The findings of this study indicate that there is an optimal growth temperature to suppress APDs with minimal thickness by affecting the APB energetics and favoring propagation along higher-index planes over {110} planes.

Conflict of interest

Authors C.S.C. Barrett, E.L. Kennon, and K.S. Jones have received research grants from Applied Materials, Inc., and K.S. Jones has consulted for Applied Materials.

Acknowledgements

This work is funded through a research grant by Applied Materials. The authors acknowledge the Major Analytical Instrumentation Center and the Nanoscale Research Facility at the University of Florida for the use of their sample preparation and characterization facilities and Dr. Simon Phillpot at the University of Florida for his thoughtful discussions.

References

[1] J.A. del Alamo, Nanometre-scale electronics with III–V compound semiconductors, Nature 479 (2011) 317–323, http://dx.doi.org/10.1038/nature10677.
[2] S.F. Fang, K. Adomi, S. Iyer, H. Morkoç, H. Zabel, C. Choi, N. Otsuka, Gallium arsenide and other compound semiconductors on silicon, J. Appl. Phys. 68 (1990) R31–R58, http://dx.doi.org/10.1063/1.346284.
[3] H. Kawanami, Heteroepitaxial technologies of III–V on Si, Sol. Energy Mater. Sol. Cells 66 (2001) 479–486, http://dx.doi.org/10.1016/S0927-0248(00)00209-9.
[4] Y. Bolkhovityanov, O.P. Pchelyakov, III–V compounds-on-Si: Heterostructure fabrication, application and prospects, Open Nanosci. J. 3 (2009) 20–33.
[5] S. Datta, G. Dewey, J.M. Fastenau, M.K. Hudait, D. Loubychev, W.K. Liu, M. Radosavljevic, W. Rachmady, R. Chau, Ultrahigh-Speed 0.5 V supply voltage In0.7 Ga0.3As quantum-well transistors on Silicon substrate, IEEE Electron Device Lett. 28 (2007) 685–687, http://dx.doi.org/10.1109/LED.2007.902078.
[6] J. Yang, P. Bhattacharya, Z. Mi, High-Performance In0.5Ga0.5As/GaAs quantum-dot lasers on Silicon with multiple-layer quantum-dot dislocation filters, IEEE Trans. Electron Devices 54 (2007) 2849–2855, http://dx.doi.org/10.1109/TED.2007.906928.
[7] T. Sakamoto, G. Hashiguchi, Si(001)−2 × 1 single-domain structure obtained by high temperature annealing, Jpn. J. Appl. Phys. 25 (1986) L78, http://dx.doi.org/10.1143/JJAP.25.L78.
[8] R.J. Hamers, R.M. Tromp, J.E. Demuth, Scanning tunneling microscopy of Si (001), Phys. Rev. B. 34 (1986) 5343–5357, http://dx.doi.org/10.1103/PhysRevB.34.5343.
[9] D.E. Aspnes, J. Ihm, Biatomic Steps on (001) Silicon Surfaces, Phys. Rev. Lett. 57 (1986) 3054–3057, http://dx.doi.org/10.1103/PhysRevLett.57.3054.
[10] M. Grundmann, Observation of the first-order phase transition from single to double stepped Si (001) in metalorganic chemical vapor deposition of InP on Si, J. Vac. Sci. Technol. B Microelectron. Nanometer Struct. 9 (1991) 2158, http://dx.doi.org/10.1116/1.585757.
[11] D. Vanderbilt, C. Lee, Energetics of antiphase boundaries in GaAs, Phys. Rev. B. 45 (1992) 11192–11201, http://dx.doi.org/10.1103/PhysRevB.45.11192.
[12] O. Rubel, S.D. Baranovskii, Formation energies of antiphase boundaries in GaAs and GaP: an ab initio study, Int. J. Mol. Sci. 10 (2009) 5104–5114, http://dx.doi.org/10.3390/ijms10125104.
[13] S.N.G. Chu, S. Nakahara, S.J. Pearton, T. Boone, S.M. Vernon, Antiphase domains in GaAs grown by metalorganic chemical vapor deposition on silicon-on-insulator, J. Appl. Phys. 64 (1988) 2981, http://dx.doi.org/10.1063/1.341561.
[14] O. Ueda, T. Soga, T. Jimbo, M. Umeno, Direct evidence for self-annihilation of antiphase domains in GaAs/Si heterostructures, Appl. Phys. Lett. 55 (1989) 445–447, http://dx.doi.org/10.1063/1.101870.
[15] A. Georgakilas, P. Panayotatos, J. Stoemenos, J.-L. Mourrain, A. Christou, Achievements and limitations in optimized GaAs films grown on Si by molecular-beam epitaxy, J. Appl. Phys. 71 (1992) 2679, http://dx.doi.org/10.1063/1.351041.
[16] V.I. Vdovin, M.G. Mil'vidskii, T.G. Yugova, Antiphase boundaries in GaAs layers on Si and Ge, J. Cryst. Growth. 132 (1993) 477–482, http://dx.doi.org/10.1016/0022-0248(93)90075-8.
[17] A. Georgakilas, J. Stoemenos, K. Tsagaraki, P. Komninou, N. Flevaris, P. Panayotatos, A. Christou, Generation and annihilation of antiphase domain boundaries in GaAs on Si grown by molecular beam epitaxy, J. Mater. Res. 8 (1993) 1908–1921, http://dx.doi.org/10.1557/JMR.1993.1908.
[18] I. Németh, B. Kunert, W. Stolz, K. Volz, Heteroepitaxy of GaP on Si: correlation of morphology, anti-phase-domain structure and MOVPE growth conditions, J. Cryst. Growth. 310 (2008) 1595–1601, http://dx.doi.org/10.1016/j.jcrysgro.2007.11.127.
[19] K. Volz, A. Beyer, W. Witte, J. Ohlmann, I. Németh, B. Kunert, W. Stolz, GaP-nucleation on exact Si (0 0 1) substrates for III/V device integration, J. Cryst. Growth. 315 (2011) 37–47, http://dx.doi.org/10.1016/j.jcrysgro.2010.10.036.
[20] C.S.C. Barrett, A.G. Lind, X. Bao, Z. Ye, K.Y. Ban, P. Martin, E. Sanchez, Y. Xin, K. S. Jones, Quantitative correlation of interfacial contamination and antiphase domain boundary density in GaAs on Si(100), J. Mater. Sci. 51 (2015) 449–456, http://dx.doi.org/10.1007/s10853-015-9334-0.
[21] M. Akiyama, Y. Kawarada, T. Ueda, S. Nishi, K. Kaminishi, Growth of high quality GaAs layers on Si substrates by MOCVD, J. Cryst. Growth. 77 (1986) 490–497, http://dx.doi.org/10.1016/0022-0248(86)90342-8.
[22] D.K. Biegelsen, F.A. Ponce, A.J. Smith, J.C. Tramontana, Initial stages of epitaxial growth of GaAs on (100) silicon, J. Appl. Phys. 61 (1987) 1856–1859, http://dx.doi.org/10.1063/1.338029.
[23] Y. Chriqui, L. Largeau, G. Patriarche, G. Saint-Girons, S. Bouchoule, I. Sagnes, D. Bensahel, Y. Campidelli, O. Kermarrec, Direct growth of GaAs-based structures on exactly (001)-oriented Ge/Si virtual substrates: reduction of the structural defect density and observation of electroluminescence at room temperature under CW electrical injection, J. Cryst. Growth. 265 (2004) 53–59, http://dx.doi.org/10.1016/j.jcrysgro.2004.01.038.
[24] C.A. Schneider, W.S. Rasband, K.W. Eliceiri, NIH Image to ImageJ: 25 years of image analysis, Nat. Methods., 9, (2012) 671–675, http://dx.doi.org/10.1038/nmeth.2089.
[25] J. Tafto, J.C.H. Spence, A simple method for the determination of structure-factor phase relationships and crystal polarity using electron diffraction, J. Appl. Crystallogr. 15 (1982) 60–64, http://dx.doi.org/10.1107/s0021889882011352.
[26] T.S. Kuan, C.-A. Chang, Electron microscope studies of a Ge–GaAs superlattice grown by molecular beam epitaxy, J. Appl. Phys. 54 (1983) 4408–4413, http://dx.doi.org/10.1063/1.332688.
[27] J.B. Posthill, J.C.L. Tarn, K. Das, T.P. Humphreys, N.R. Parikh, Observation of antiphase domain boundaries in GaAs on silicon by transmission electron microscopy, Appl. Phys. Lett. 53 (1988) 1207, http://dx.doi.org/10.1063/1.100021.
[28] I. Németh, B. Kunert, W. Stolz, K. Volz, Ways to quantitatively detect antiphase disorder in GaP films grown on Si(001) by transmission electron microscopy, J. Cryst. Growth 310 (2008) 4763–4767, http://dx.doi.org/10.1016/j.jcrysgro.2008.07.105.
[29] A.C. Lin, M.M. Fejer, J.S. Harris, Antiphase domain annihilation during growth of GaP on Si by molecular beam epitaxy, J. Cryst. Growth 363 (2013) 258–263, http://dx.doi.org/10.1016/j.jcrysgro.2012.10.055.
[30] A. Beyer, I. Németh, S. Liebich, J. Ohlmann, W. Stolz, K. Volz, Influence of crystal polarity on crystal defects in GaP grown on exact Si (001), J. Appl. Phys. 109 (2011) 83529, http://dx.doi.org/10.1063/1.3567910.
[31] A. Beyer, B. Haas, K.I. Gries, K. Werner, M. Luysberg, W. Stolz, K. Volz, Atomic structure of (110) anti-phase boundaries in GaP on Si(001), Appl. Phys. Lett. 103 (2013) 32107, http://dx.doi.org/10.1063/1.4815985.
[32] S.H. Vajargah, S.Y. Woo, S. Ghanad-Tavakoli, R.N. Kleiman, J.S. Preston, G. A. Botton, Atomic-resolution study of polarity reversal in GaSb grown on Si by scanning transmission electron microscopy, J. Appl. Phys. 112 (2012) 93101, http://dx.doi.org/10.1063/1.4759160.